Comparison of ALE and SPH Simulations of Vertical Drop Tests of a Composite Fuselage Section into Water

Karen E. Jackson and Yvonne T. Fuchs
NASA Langley Research Center
Hampton, VA

Abstract

Simulation of multi-terrain impact has been identified as an important research area for improved prediction of rotorcraft crashworthiness within the NASA Subsonic Rotary Wing Aeronautics Program on Rotorcraft Crashworthiness. As part of this effort, two vertical drop tests were conducted of a 5-ft-diameter composite fuselage section into water. For the first test, the fuselage section was impacted in a baseline configuration without energy absorbers. For the second test, the fuselage section was retrofitted with a composite honeycomb energy absorber. Both tests were conducted at a nominal velocity of 25-ft/s. A detailed finite element model was developed to represent each test article and water impact was simulated using both Arbitrary Lagrangian Eulerian (ALE) and Smooth Particle Hydrodynamics (SPH) approaches in LS-DYNA®, a nonlinear, explicit transient dynamic finite element code. Analytical predictions were correlated with experimental data for both test configurations. In addition, studies were performed to evaluate the influence of mesh density on test-analysis correlation.

Introduction

Since its inception in 2006, the NASA Subsonic Rotary Wing (SRW) Aeronautics Program in Rotorcraft Crashworthiness [1] has focused attention on two main areas of research: development of a Deployable Energy Absorber (DEA) concept and improved prediction of rotorcraft crashworthiness. The DEA concept is a composite honeycomb structure that can be deployed to provide energy attenuation, much like an external airbag system. Over the past two years, research has been conducted to develop the concept through component and full-scale testing, to evaluate various deployment techniques, and to demonstrate its potential as an energy attenuator during multi-terrain impacts [2, 3].

The second main research area relates to crash modeling and simulation. Commercial nonlinear, explicit transient dynamic finite element codes, such as LS-DYNA® [4], are capable of accurately simulating airframe structural response to crash impact. However, analytical models need to be thoroughly validated so that designers have greater confidence in the analytical results, thus encouraging use of crash simulation during preliminary design. A Workshop on Computational Methods for Crashworthiness was held on September 2-3, 1992, at NASA Langley Research Center, Hampton, Virginia [5]. Attendees were asked to identify key technology needs for improved crash modeling and simulation which were grouped under five main headings including (1) understanding the physical phenomena associated with crash events, (2) high-fidelity modeling of the vehicle and the occupant during crash, (3) efficient computational strategies, (4) test methods, measurement techniques, and scaling laws, and (5) validation of numerical simulations. Many of the key technology needs identified during the workshop are still valid today. Consequently, the current SRW research program plans to address many of these topic areas. Specifically, research directed toward improved prediction of rotorcraft crashworthiness will focus on occupant modeling and injury prediction, multi-terrain impact simulation, model validation studies that focus on probabilistic analysis, and development of system-integrated simulation models.

Impact testing and simulation to understand the multi-terrain dynamic response of airframe structures is an important research area. Accident data indicate that more than 80% of helicopter crashes occur on multi-terrain surfaces such as water, soft soil, plowed or grassy fields, and shallow swamps, as opposed to smooth prepared surfaces [6]. In addition, research studies have shown that helicopters, designed for crash resistance onto hard surfaces, do not perform well during multi-terrain impacts [7-12]. For hard surface impacts, load is transferred to the stiffest part of the helicopter subfloor structure, which is typically keel beams and fuselage frame structures. However, in water or soft soil impact, the primary mode of loading is pressure applied to the outer skin. These differences are depicted in Figure 1. In typical frame-stringer construction, the unsupported outer skin can easily rupture during water impact allowing rapid water ingress. Also, based on a systems approach to crashworthiness, many helicopters rely on energy attenuating landing gear for improved crash protection. However, landing and skid gear are completely ineffective as energy absorbers during water impact. Thus, future requirements for multi-terrain crash resistance would increase the need for novel energy absorbing structural design concepts. In addition, external devices such as air bag systems could be used to augment the crash performance of helicopters during impact. Based on this information, the NASA SRW research program has focused attention on both multi-terrain impact simulation and evaluation of the composite honeycomb DEA concept. In 2006-2007, vertical impact tests and simulations were performed onto concrete, water, and soft soil of a composite fuselage section that was retrofitted with the DEA concept, as reported in References 2 and 13. This paper will document the water impact testing and simulation.

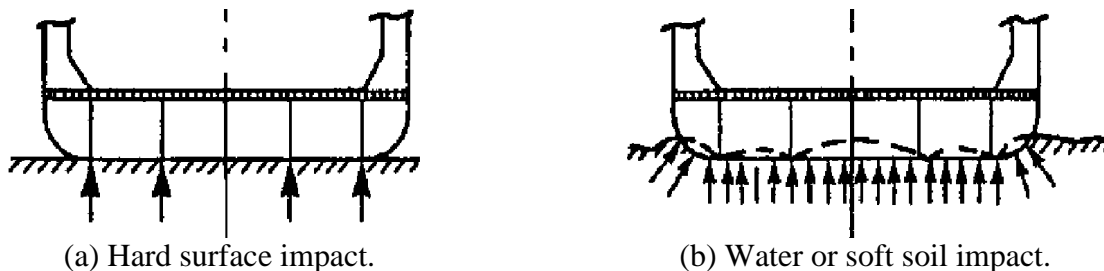(a) Hard surface impact.   (b) Water or soft soil impact.

Figure 1. Schematics illustrating impact loading for hard surface and water impacts.

In 2007, two vertical drop tests were conducted into water of a composite fuselage section, with and without the DEA concept. The objectives of the tests were twofold: to demonstrate the energy absorption capabilities of the DEA for water impact and to provide experimental data for model validation. A detailed finite element model was developed to represent each test article and the water impacts were simulated using both Arbitrary Lagrangian Eulerian (ALE) and Smooth Particle Hydrodynamics (SPH) approaches in LS-DYNA [4, 14]. Using the ALE formulation, the aircraft structure is modeled using a purely Lagrangian mesh composed of deformable elements with associated nodes that move with the element. The fluid, or water, is typically modeled using a stationary Eulerian mesh in which the fluid material flows, while conserving mass, momentum, and energy. When using the ALE algorithm, a portion of the air volume above the water must also be modeled with an Eulerian mesh to allow wave formation and movement, thus simulating the water splash. Coupling of the Lagrangian and Eulerian meshes to solve the fluid-structure interaction problem is accomplished by using the *CONSTRAINED_LAGRANGE_IN_SOLID command in LS-DYNA. With the SPH technique, both the structure and fluid can be modeled using a Lagrangian approach. The SPH technique utilizes a meshless Lagrangian method to represent fluids. In the SPH method, the fluid material

is treated as particles that have their masses smoothed in space. Coupling between the SPH grid points and the structural model is accomplished through normal contact definitions.

This paper will provide an overview of the experimental program including a description of the DEA concept and a summary of the drop tests performed onto water. The development of the ALE and SPH models will be discussed in detail along with test-analysis correlation. For both types of fluid-structure interaction models, mesh sensitivity studies were conducted, and these results will also be presented.

Experimental Program

This section of the paper will give a brief description of the DEA concept and will summarize the vertical drop tests of the composite fuselage section into water, the first conducted on the fuselage section in a baseline configuration without the DEA and the second conducted on the fuselage section retrofitted with the DEA.

Description of the DEA

The DEA concept utilizes an expandable honeycomb-like structure to absorb impact energy by crushing. The concept is based on a unique and patented flexible hinge at each junction of its cell walls. This feature enables considerable variability in the size and strength of the energy absorbers that can be fabricated and deployed [2, 3]. Like conventional honeycomb, once expanded, the energy absorber is transformed into an efficient orthotropic cellular structure, with greater strength and stiffness along the cell axis as compared to the transverse directions. The flexible hinge enables various methods of expanding the cellular structure. The linear expansion mode, shown in Figure 2(a), represents the simplest mode. When expanded in this fashion, the DEA produces higher specific energy absorption due to a more efficient volumetric expansion (lower effective expanded density). However, radial deployment, which is illustrated in Figure 2(b), produces an energy absorber with better omni-directional capability. Because most practical applications involve curved rather than flat surfaces, the two basic deployment methods can be combined into a hybrid approach.
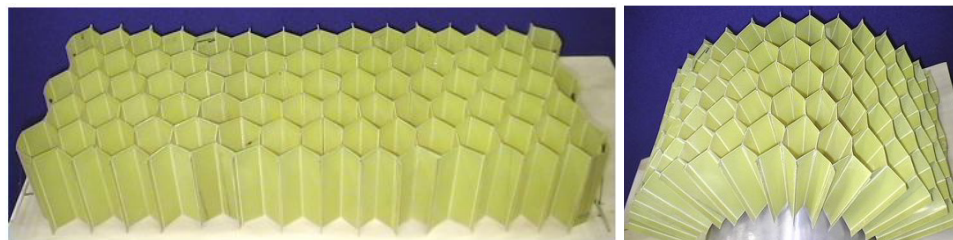
(a) Linear deployment.   (b) Radial deployment.

Figure 2. Photographs showing deployment methods of the DEA.

Typical results from an impact test are shown in Figure 3. For this test, a steel block weighing 477.2-lb impacted a 104-cell DEA component at 22.2-ft/s. The DEA was fabricated of Kelvar™-129 fabric with a ±45° orientation relative to the vertical or loading direction. Nominal cell width was 1.0-in. and cell wall thickness was 0.01-in. The DEA was 10-in. high, 21-in. long, and 15.75-in. wide, and was designed to achieve an average crush stress of 20-psi. Dynamic crush stress versus stroke response is plotted in Figure 3(a). An average crush stress of 20.5-psi was obtained over a crush stroke of 60%. Typical stroke efficiencies of between 75 and 85% are

observed for fully compressed DEA components. Note that the area under the curve shown in Figure 3(a) is proportional to the amount of kinetic energy dissipated through crushing of the energy absorber. A post-test photograph, shown in Figure 3(b), depicts the deformation modes exhibited by the DEA during crushing. The primary mechanisms for energy dissipation are local buckling, tearing, and delamination.
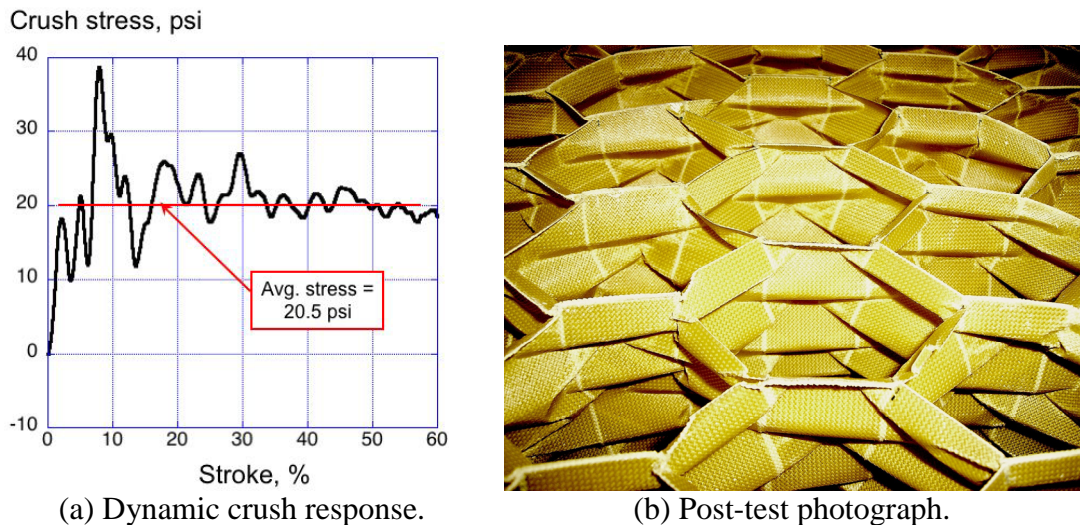

(a) Dynamic crush response.　　　　　　(b) Post-test photograph.

Figure 3. Test data for deployable honeycomb specimen.

Water Impact Tests

Two full-scale drop tests were conducted of a 5-ft-diameter, 5-ft-long composite fuselage section to evaluate the energy absorption capabilities of the DEA during water impact. Pre-test photographs of the two test articles are shown in Figure 4. The composite fuselage section was developed during a prior research program [15] at NASA Langley Research Center and has been used as a test bed to evaluate the responses of seats and dummies [16], to study quantitative correlation methods including experimental uncertainty [17], and to examine the influence of multi-terrain impact surfaces [18]. The fuselage section is fabricated using composite sandwich construction. The upper fuselage cabin is fabricated using a 3-lb/ft^3 polyurethane closed-cell foam with E-glass/epoxy fabric face sheets, while the floor is fabricated using 8-lb/ft^3 polyurethane closed-cell foam with hybrid E-glass/epoxy and graphite/epoxy fabric face sheets. The layers of graphite/epoxy fabric and the higher density foam were used for increased stiffness and improved structural rigidity of the floor, which is designed to serve as primary, load-bearing structure. As such, the floor must react the loads generated by crushing of subfloor energy absorbers or external energy attenuating systems.

The vertical drop tests were performed by releasing the test articles to impact a 15-ft-diameter pool of water (approximately 42-in. deep) that was placed at the base of the 70-ft drop tower at NASA Langley. The fuselage section without energy absorbers, shown in Figure 4(a), was tested first to provide a datum for comparison with the second test, which included four deployable honeycomb energy absorbers, as shown in Figure 4(b). The energy absorbers were made of a single woven-ply of Kevlar™-129, had a cell width equal to 1.0-in., and weighed 5.6-lb each. The deployed size of the honeycomb was 20-in. tall, 16.5-in. wide and 20.5-in. deep and incorporated a curved surface (18-in. radius) on the bottom. The curved surface was intended to attenuate the peak load at initial impact. Each energy absorber was fitted with a cover, fabricated

of a single ply of Kevlar™-129 fabric that was incorporated into the design of the structure. A close-up photograph highlighting the cover is shown in Figure 5.   The energy absorbers were located as close to the edge of the flat portion of the floor as possible and were mounted symmetrically about the mid-surface and centerline of the section.

(a) Fuselage section without energy absorbers.   (b) Fuselage section with energy absorbers.

Figure 4. Pre-test photographs of the test articles.

Figure 5. Close-up photograph showing the cover over the DEA block.

Each fuselage section contained ten 100-lb lead blocks that were mounted, five per side, to the floor of the fuselage section using standard seat rail fasteners. Accelerometers (250-g maximum range) were mounted on the lead blocks to record the dynamic structural response of the floor, as indicated in the floor plan schematics of Figure 6. For the drop test of the fuselage section without energy absorbers, only two accelerometers were used, one each on the right and left center lead blocks, as shown in Figure 6(a). For the test of the fuselage section with energy absorbers, eight accelerometers were used, as indicated in Figure 6(b). For this test, the right center lead block was covered with an aluminum plate, which caused anomalous behavior in the attached accelerometers. Consequently, the analytical correlations shown in this paper are for the accelerometer located on the far left center lead block. Also, note that for brevity of the paper and because only center accelerometers were used in the drop test without DEA, correlation with the front and rear accelerometer data for the test with the DEA is not shown. Data were collected at 10,000 samples per second for both impact tests. For the purposes of this

paper, all analytical and experimental data have been filtered using an SAE J211 filter with a Channel Filter Class (CFC) 180 [19]. The total weights of the fuselage sections, with and without energy absorbers, were 1,200-lb and 1,225-lb, respectively. The measured velocities at impact were 24.7- and 25.0-ft/s for the test with and without energy absorbers, respectively.
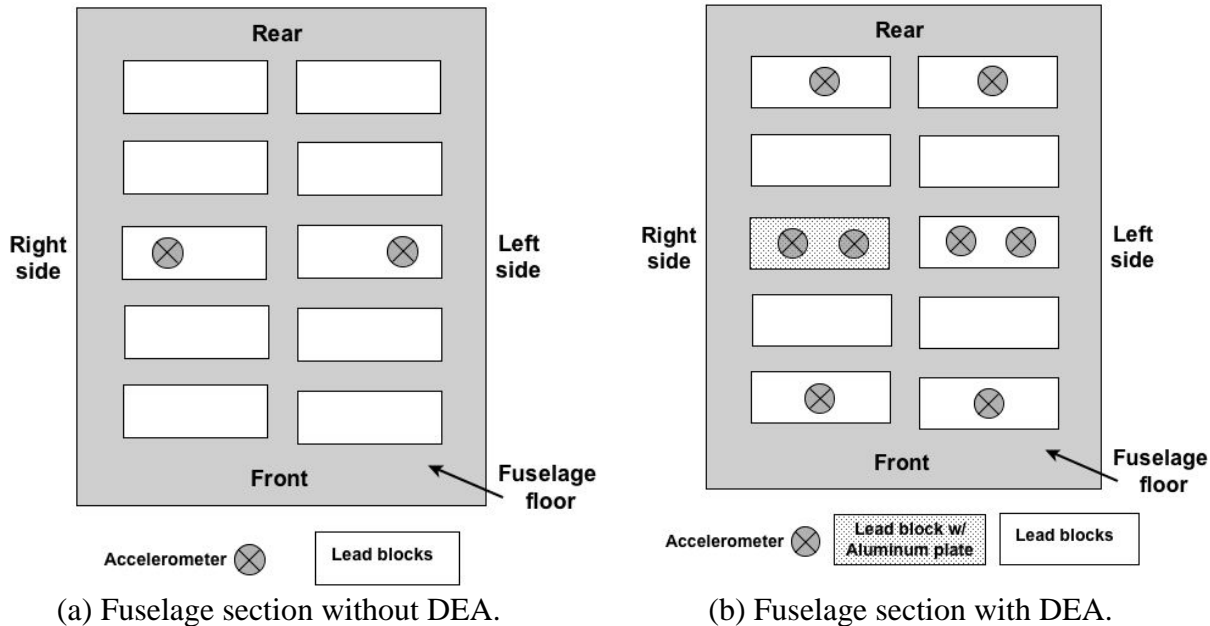

(a) Fuselage section without DEA.   (b) Fuselage section with DEA.

Figure 6. Instrumentation plans for two fuselage section drop tests.

During the water drop test of the fuselage section without energy absorbers, the measured peak accelerations ranged from 150- to 220-g's with a slight time shift between peaks. Based on these results, it was determined that the fuselage section impacted the water with a slight 1°-rolled attitude. The only post-test damage to the fuselage section consisted of a minor delamination of a single E-glass/epoxy face sheet. This damage was repaired prior to the second drop test with energy absorbers.

The results of the water impact test of the fuselage section with DEA indicated an average peak acceleration of 20-g on the floor. The data also showed that the fuselage section impacted the water with a 1°-rolled attitude. Less than 1-in. of crush of the energy absorbers was observed post-test, which indicates that energy attenuation was achieved by momentum transfer to the water, rather than from honeycomb crushing. The peak acceleration was reduced significantly in comparison to the test without DEA. This reduction is attributed to the reduced cross-sectional area and the curved bottom surfaces of the DEA in comparison with the flat bottom of the fuselage floor.

LS-DYNA Simulation of Water Impact

Both test configurations were simulated in LS-DYNA, version 971, using the ALE and SPH methods for solving fluid-structure interaction problems. Model development and test-analysis correlations for each method will be described in separate subsections. Since the same fuselage section models were used in both the ALE and SPH simulations, the development of the Lagrangian finite element models of the two test articles is discussed, as follows.

Lagrangian Models of Two Fuselage Section Configurations
The Lagrangian model of the fuselage section without energy absorbers, shown in Figure 7(a), consists of 48,724 nodes; 25,522 elements including 10,388 shells, 14,946 solids, and 188 beams; and 40 concentrated masses. The model of the fuselage section with energy absorbers, shown in Figure 7(b), contains an additional 28,696 nodes and 24,128 solid elements to represent the DEA. In both models, the inner and outer face sheets of the upper section and floor were modeled using shell elements, and the foam cores in the upper section and floor were represented by hexagonal solid elements. The seat tracks were modeled using beam elements and the lead blocks were represented using four concentrated mass elements per block.

The material properties of the E-glass/epoxy and graphite/epoxy fabric materials were determined from coupon tests and were modeled using *MAT_PLASTIC_KINEMATIC, a linear elastic-plastic material model in LS-DYNA with strain hardening. The 3- and 8-lb/ft^3 polyurethane foam cores in the upper section and floor were represented using a *MAT_FU_CHANG_FOAM material model. The foam properties were obtained from compression tests of individual blocks of foam, without face sheets. Additional details of the model development may be found in Reference 15.

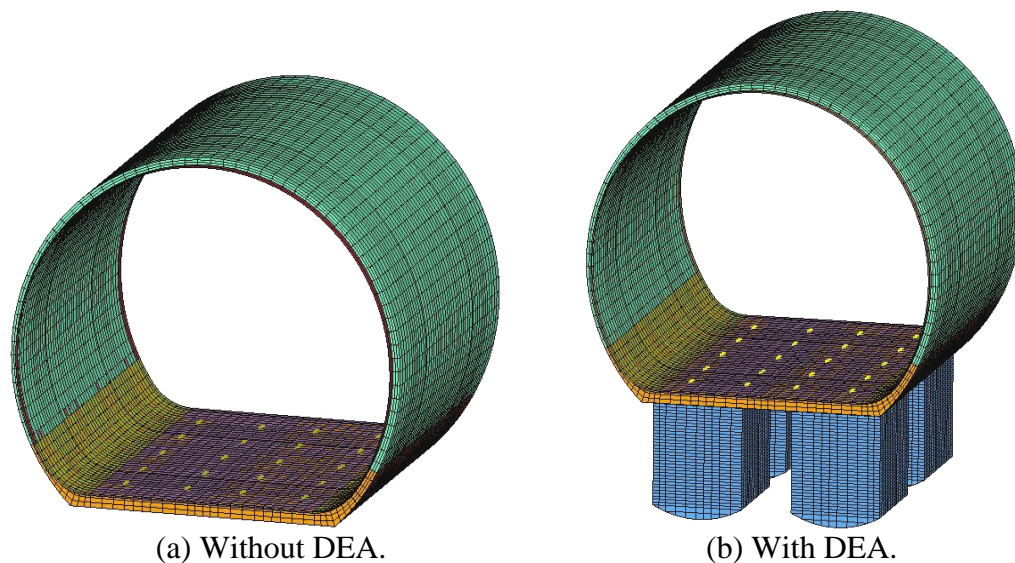(a) Without DEA.   (b) With DEA.

Figure 7. Finite element models of the two fuselage section configurations.

For this preliminary analysis, the composite honeycomb energy absorbers were modeled simply using solid elements, as shown in Figure 7(b). The elements were assigned a *MAT_CRUSHABLE_FOAM material property with a user-defined crush stress versus strain response, shown in Figure 8, that was determined based on the test data provided in Figure 3(a). A *MAT_ADD_EROSION card was defined to eliminate elements that exceeded a volumetric strain of 85%. Note that the stress response, shown in Figure 8, begins to increase dramatically after 80% strain, which represents the compaction response of the energy absorber.

ALE Simulation: Water Impact of the Fuselage Section Without Energy Absorbers
Pre-test predictions were generated for the 25-ft/s vertical impact of the fuselage section without energy absorbers into water based on ALE capabilities in LS-DYNA. The complete model is shown in Figure 9(a). The Euler region consists of a cylindrical tank of water with a cylindrical

volume of air above the water that was represented using 72,900 solid elements. Pre-test predictions were obtained assuming a perfectly flat impact. The simulation required 13 hours and 35 minutes to simulate 0.05-s on a single processor workstation computer. Predicted peak accelerations for the center lead blocks averaged 182-g's, which falls within the measured range of 150- to 220-g's, as shown in Figure 9(b). Following the test, the ALE model was re-executed with the fuselage section rolled by 1°. The analytical responses for this model exactly predict the magnitude and timing of the peak accelerations obtained from the test, as shown in Figure 10. However, the onset rate of the acceleration response is not well predicted. It should be noted that the acceleration onset rate may be influenced by the fact that damped accelerometers were used and that the accelerometers were mounted directly to a 100-lb. lead mass, thus providing additional structural damping.
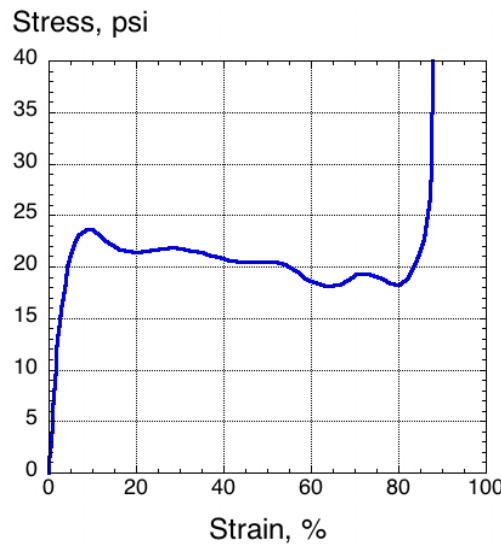
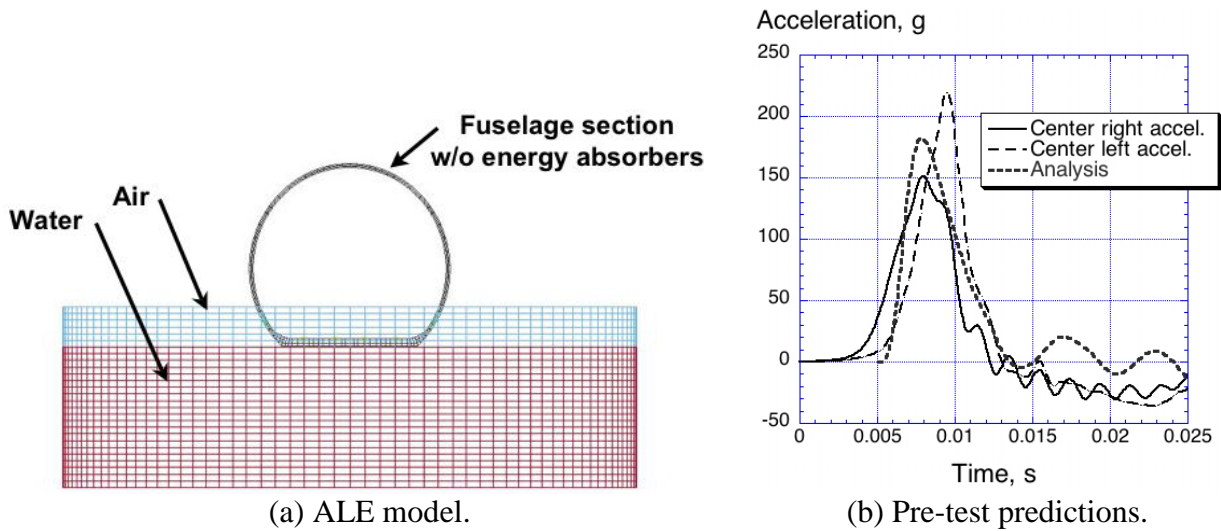Figure 8. Stress-strain response of the DEA.

(a) ALE model.

(b) Pre-test predictions.

Figure 9. ALE model of fuselage section without energy absorbers and pre-test predictions.

(a) Left center block.   (b) Right center block.
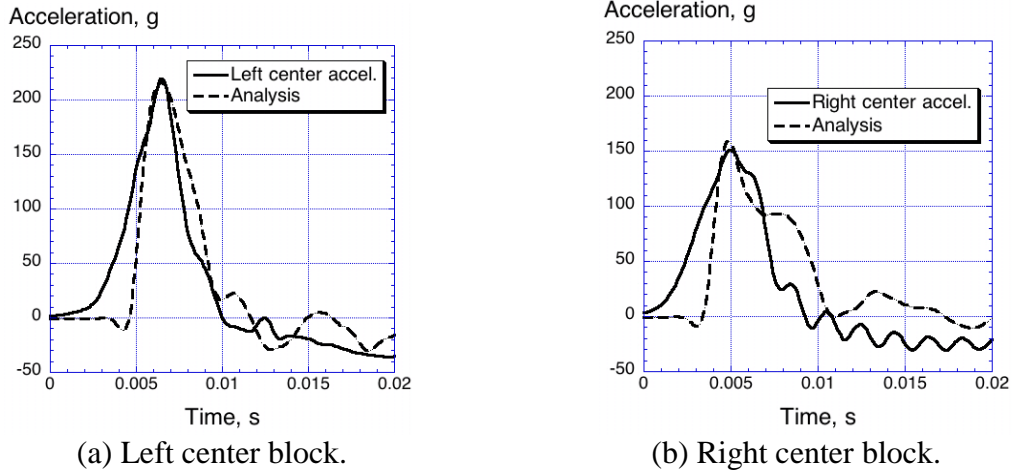
Figure 10. Post-test correlation of 1°-rolled model.

ALE Simulation: Water Impact of the Fuselage Section With Energy Absorbers
The LS-DYNA model of the fuselage section was modified to include the four blocks of the DEA, as shown in Figure 11(a). The model was executed, assuming a flat impact, to generate pre-test predictions of floor-level accelerations. The simulation required 13 hours and 6 minutes to simulate 0.05-s on a single processor workstation computer. The ALE cylindrical mesh of air and water was the same as shown in Figure 9(a). A comparison of pre-test analytical predictions and test data is plotted in Figure 11(b). Only data from the center left accelerometer is shown, since anomalous data were obtained from the center right accelerometers. The simulation over predicted the peak acceleration (20-g for the analysis versus 16.9-g for the test). In addition, the pulse duration of the predicted response was shorter than the test.

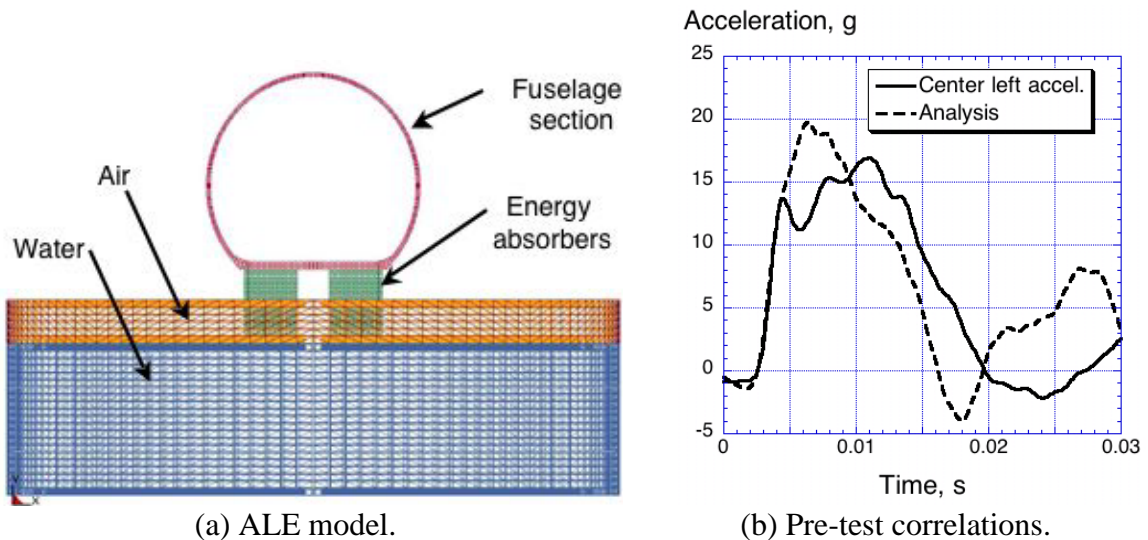(a) ALE model.   (b) Pre-test correlations.

Figure 11. ALE model and pre-test predictions correlated with test data.

As noted previously, the fuselage section with the deployable energy absorbers impacted the water with a 1°-rolled attitude. Following the test, the fuselage section model, shown in Figure 11(a), was rotated by 1° and re-executed. The test-analysis correlation for this simulation is shown in Figure 12.   The predicted response matches the peak acceleration (17.5-g for the

analysis compared with 16.9-g for the test) and the pulse duration; however, the onset rate of acceleration is not well predicted.
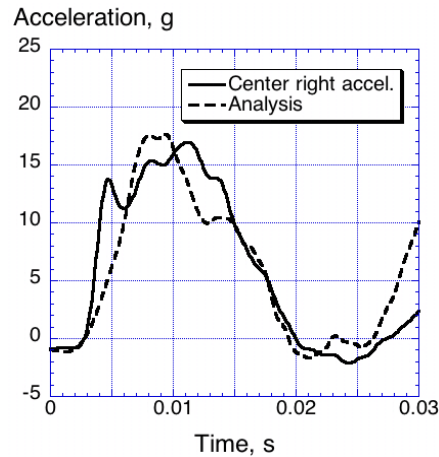

Figure 12. Post-test correlation for the 1°-rolled fuselage model.

ALE Simulation: Mesh Refinement Study

A mesh refinement study was conducted to determine the influence of mesh size on the ALE simulation results. While the density of the cylindrical mesh, shown in Figure 9(a), was not uniform, a nominal element edge length of 2.7-in. was calculated be checking node-to-node distances in the region beneath the fuselage section. For the mesh refinement study, a square-shaped 1-in. gradient mesh was used, which was identical to the mesh reported in Reference 8. For the gradient mesh, the region beneath the fuselage section contained 1-in. cubic solid elements. Two views of the model are shown in Figure 13. The total number of elements in the Eulerian gradient mesh is 90,000. For this simulation, the fuselage section model was rolled by 1° with respect to the Eulerian mesh axes. The comparison of predicted and experimental acceleration responses of the far left accelerometer located at the center of the fuselage section is shown in Figure 14. The predicted peak acceleration is 17.9-g compared with 16.9-g for the test, and the pulse duration is slightly shorter for the analysis than the test. The model required 12 hours and 17 minutes to simulate 0.05-s on a single processor workstation computer.

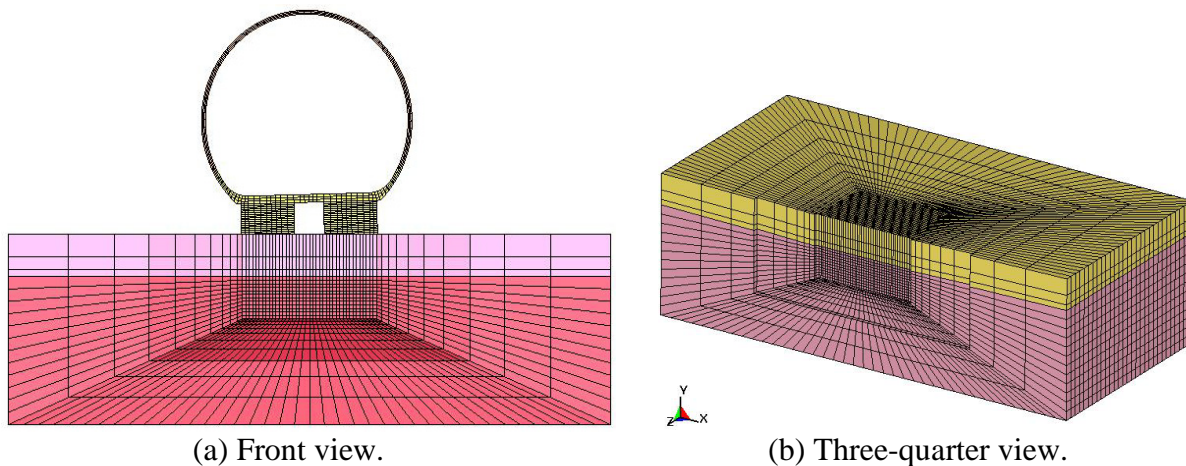(a) Front view.   (b) Three-quarter view.

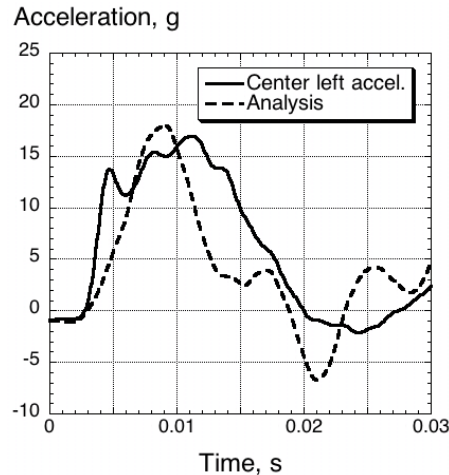Figure 13. Two views of a center-cut slice of the Euler gradient mesh.

Figure 14. Test-analysis correlation for the gradient mesh model.

Overall the level of correlation is not improved with the refined gradient mesh for the ALE simulation. This finding may be attributed to the fact that a completely new square mesh was introduced rather than refining the existing cylindrical mesh. In addition, the gradient mesh was fine in the region beneath the fuselage section, but was coarse away from the center region. A better approach would have been to refine the existing cylindrical mesh, or to use a fine, uniform mesh for the square, before moving to the more complicated gradient mesh.

SPH Simulation: Water Impact of the Fuselage Section Without Energy Absorbers

Predictions were generated for the 25-ft/s vertical impact of the fuselage section without energy absorbers into water using the SPH capabilities in LS-DYNA with 3-, 2- and 1.5-in. mesh spacing. The models are shown in Figure 15. The SPH meshes used the default parameters, namely the CSLH parameter in the *SECTION_SPH card was 1.2 for all three models. The CSLH parameter defines a constant that is applied to smoothing of the particles and can be thought of as defining the "sphere of influence" of each particle. For these simulations, the fuselage section was rolled by 1° to mimic the actual impact attitude during the test. Contact between the fuselage section and the SPH mesh was defined using the *CONTACT_AUTOMATIC_NODES_TO_SURFACE. The 3-in. mesh consisted of 56,560 SPH elements, and the simulation took 16 hours and 35 minutes to simulate 0.05-s. The 2-in. mesh consisted of 129,128 SPH elements, and the simulation took 28 hours and 32 minutes to simulate 0.05-s. Finally, the 1.5-in. mesh consisted of 305,452 SPH elements, and the simulation took 42 hours to simulate 0.031-s.

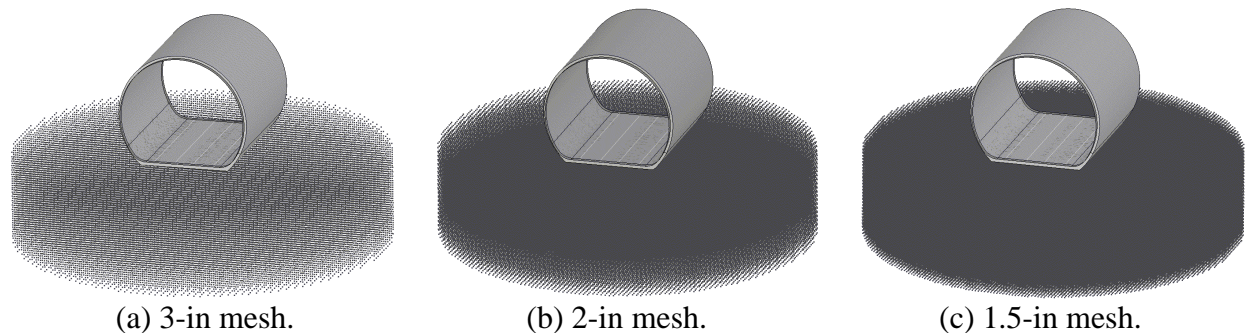(a) 3-in mesh.   (b) 2-in mesh.   (c) 1.5-in mesh.

Figure 15. SPH models of fuselage section without energy absorbers.

Comparisons of the test and analysis acceleration responses of the left and right center lead block for the 3-, 2-, and 1.5-in. mesh spacing models are presented in Figures 16-18, respectively. In general, the 3-in. mesh spacing was slightly more accurate in predicting the test results. For all models, the acceleration onset rate for the test data is much less steep than the predicted responses, likely due to the damping of the accelerometers. However, the peak acceleration differentials noted in Figures 16-18 displayed unanticipated trends, i.e. the finer meshes yielded less accurate predictions.
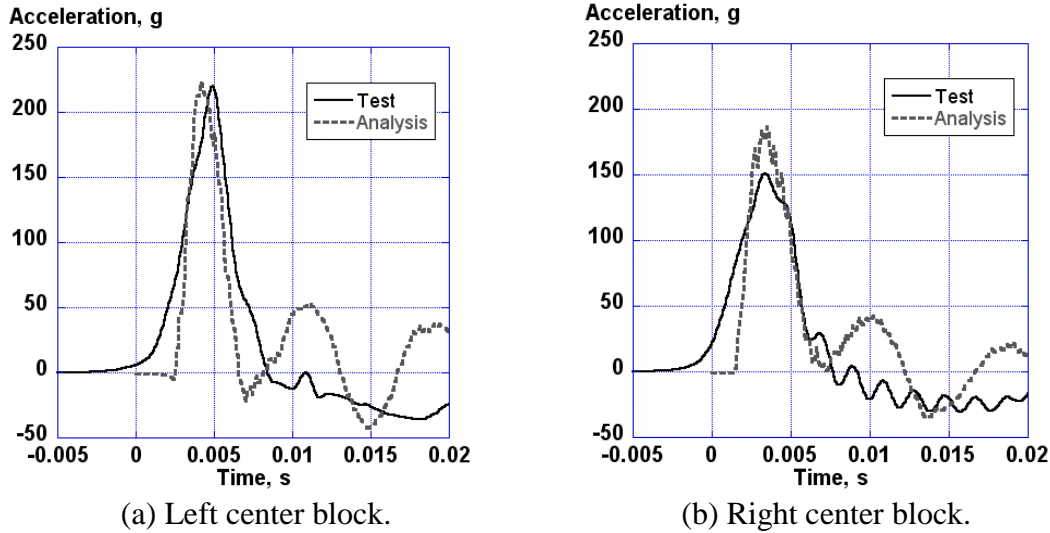
(a) Left center block.	(b) Right center block.

Figure 16. Post-test correlation of 3-in. mesh SPH model with 1°-rolled fuselage section.

(a) Left center block.	(b) Right center block.
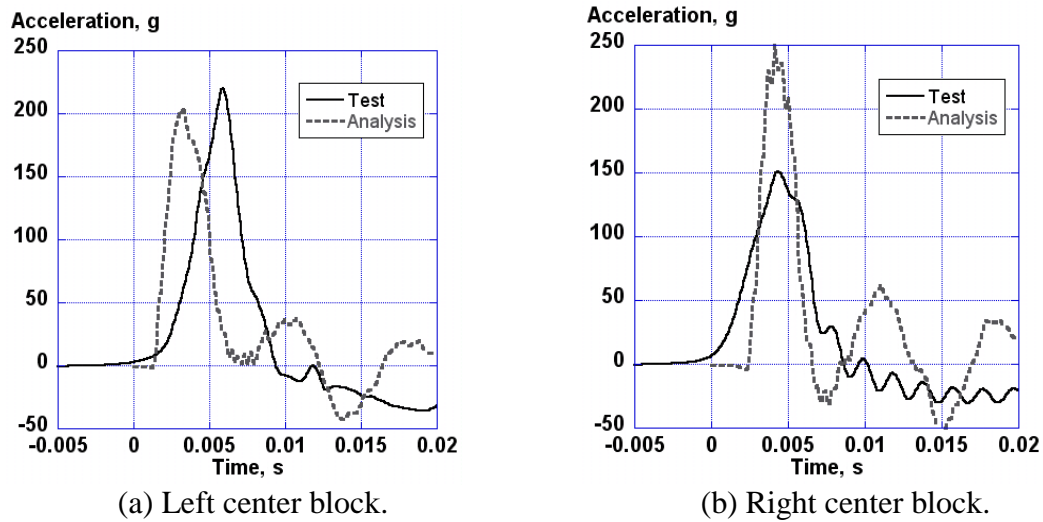
Figure 17. Post-test correlation of 2-in. mesh SPH model with 1°-rolled fuselage section.

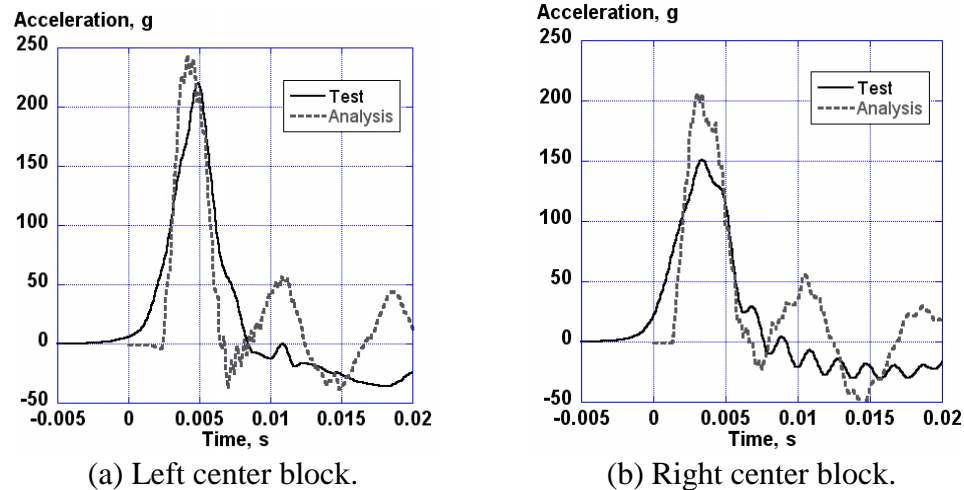(a) Left center block.   (b) Right center block.

Figure 18. Post-test correlation of 1.5-in. mesh SPH model with 1°-rolled fuselage section.

SPH Simulation: Water Impact of the Fuselage Section With Energy Absorbers
Predictions were generated for the 24.7-ft/s vertical impact of the fuselage section with energy absorbers into water using the SPH 3-, 2-, and 1.5-in. mesh spacing models. The models are shown in Figure 19. The SPH meshes were the same as used previously for the simulations of the fuselage section without DEA. However, the simulation times varied due to the increased number of elements associated with the DEA. The 3-in. mesh required 17 hours and 32 minutes to simulate 0.05-s. The 2-in. mesh took 29 hours and 6 minutes to simulate 0.05-s. The 1.5-in. mesh required 67 hours and 9 minutes to simulate 0.05-s.

The analytical predictions for the 3-, 2-, and 1.5-in. mesh SPH spacing models are shown in Figures 20(a), 20(b), and 20(c), respectively. The 3-in. model under predicts the test results, and the 1.5-in. model over predicts the tests results. Therefore, it was hoped that the 2-in. mesh spacing SPH model would correlate better with the test data, and, as Figure 20(b) indicates, the 2-in. model correlates with the test data very well.
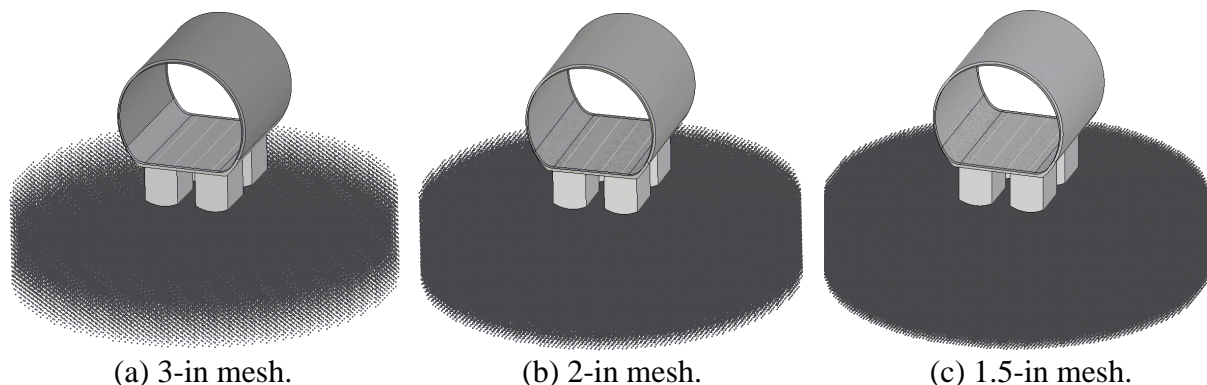

(a) 3-in mesh.   (b) 2-in mesh.   (c) 1.5-in mesh.

Figure 19. SPH models of fuselage section with energy absorbers.

(a) 3-in. spacing.   (b) 2-in. spacing.   (c) 1.5-in. spacing.
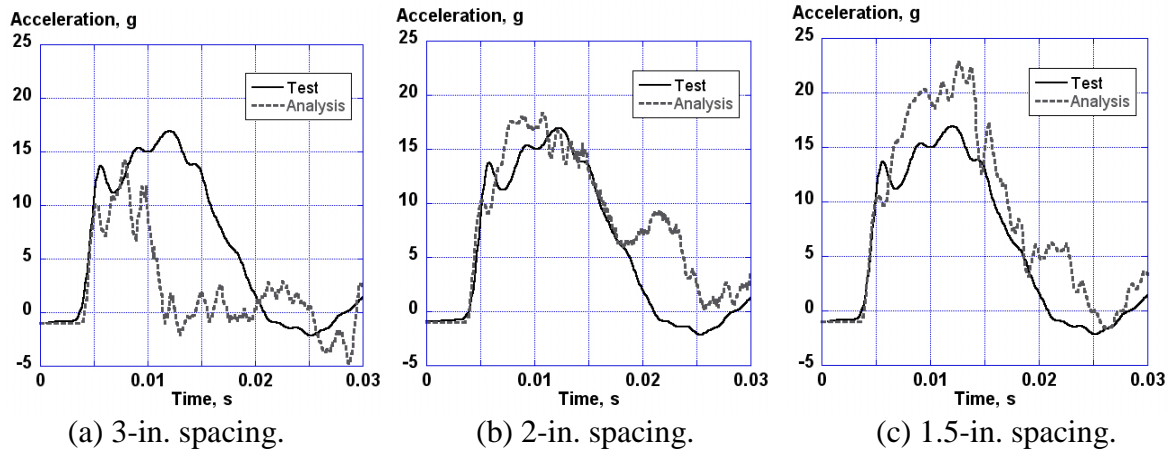
Figure 20. Post-test correlation of the fuselage with energy absorber SPH models.

SPH Simulation: Mesh Refinement Study

The results obtained from the SPH analyses yielded unexpected findings in that the finer SPH mesh did not yield the most accurate results. Consequently, a separate mesh refinement study was conducted to further investigate this behavior. In August 2001, a circular earthen dam was built and filled with water for a series of 26-in.-diameter, instrumented hemispherical penetrometer drop tests that were conducted at 25-ft/s. The penetrometer weighed 64 lb and was simulated as a rigid body. Data from these tests are used to perform a mesh sensitivity study of the penetrometer into water using the SPH capabilities in LS-DYNA. It should be noted that only the density of the SPH mesh was modified, and the 1-in. mesh discretization of the penetrometer was not varied.

Five models, shown in Figure 21, with varying SPH mesh densities were created to compare the sensitivity of the predicted response to mesh size. The model results, filtered with a SAE J211 equivalent 1000-Hz low-pass filter [19], are plotted in Figure 22 with the August 2001 test data. The SPH meshes used the default parameters, namely the CSLH parameter in the *SECTION_SPH card was 1.2 for all five models. The model with a 1.5-in. mesh, shown in Figure 21(a), consisted of 42,936 SPH elements, and the simulation took 12 minutes and 6 seconds to simulate 0.05-s. Results for this model are shown in Figure 22(a). The model with a 1-in. mesh, shown in Figure 21(b), consisted of 145,764 SPH elements, and the simulation took 58 minutes and 40 seconds to simulate 0.05-s, with corresponding results shown in Figure 22(b). The 0.75-in. mesh spacing model, shown in Figure 21(c), consisted of 346,032 SPH elements, and the simulation took 3 hours, 7 minutes, and 3 seconds to simulate 0.05-s, with corresponding results shown in Figure 22(c). The 0.6-in. SPH mesh spacing model, shown in Figure 21(d), consisted of 676,620 SPH elements, and the simulation took 7 hours, 30 minutes, and 28 seconds to simulate 0.05-s and the results are shown in Figure 22(d). Finally, the model with a 0.5-in. SPH mesh spacing, shown in Figure 21(e), consisted of 1,169,064 SPH elements, and the simulation took 15 hours, 8 minutes, and 20 seconds to simulate 0.05-s, with corresponding correlation results shown in Figure 22(e).

The results for the 1.5-, 1.0-, and 0.75-in. mesh densities clearly over predict the maximum peak acceleration, the 0.5-in. mesh spacing result is under predicted, and the predictions from the 0.6-in. mesh spacing model correlate best with the test data. This mesh density study clearly illustrates the importance of performing a mesh study using the SPH method and that it should

not be assumed that by simply refining the mesh better results will be obtained. The relationship between the refined mesh spacing and solution time is plotted in Figure 23.

(a) 1.5-inch mesh spacing.

(b) 1-inch mesh spacing.
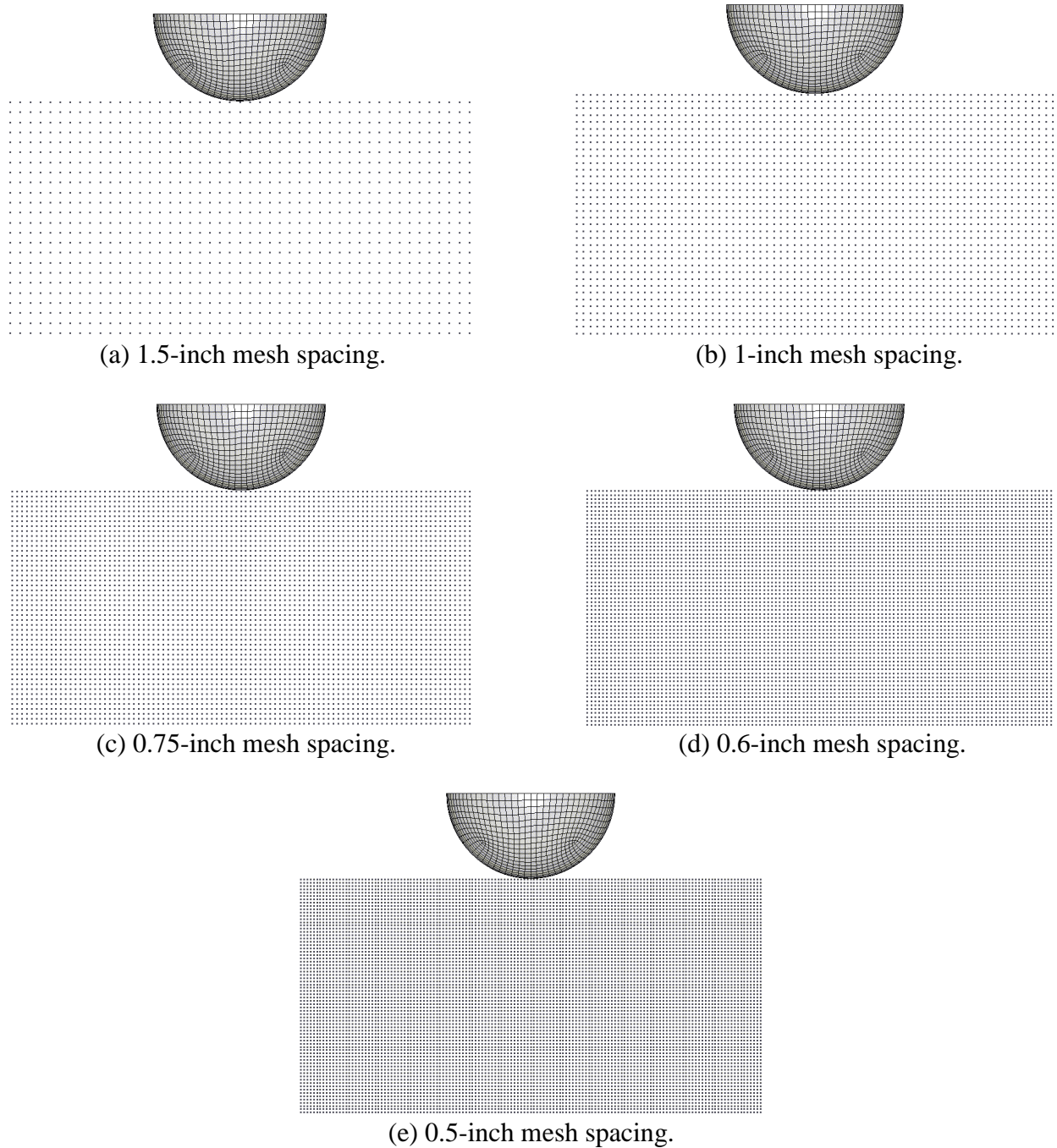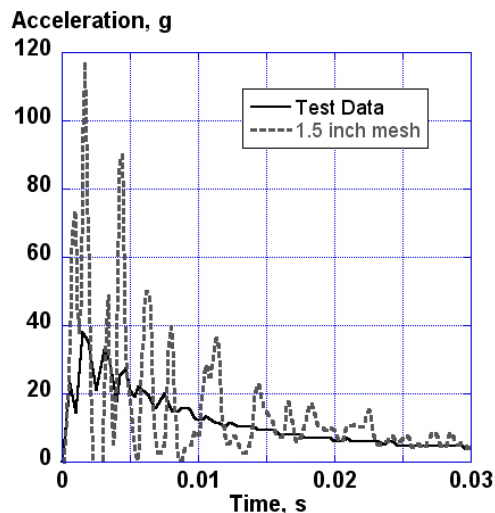

(c) 0.75-inch mesh spacing.
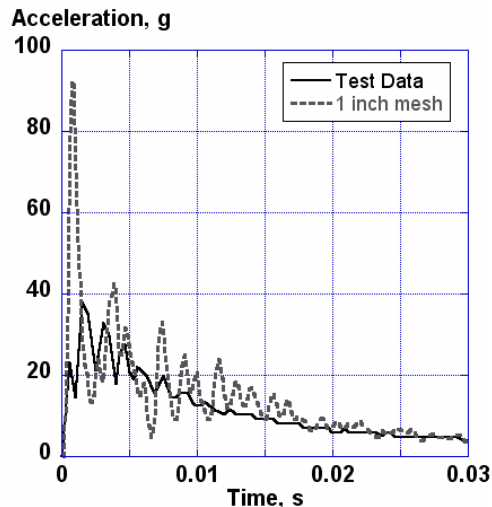

(d) 0.6-inch mesh spacing.
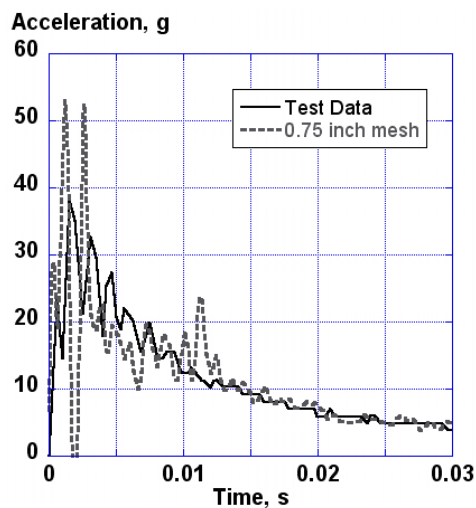

(e) 0.5-inch mesh spacing.

Figure 21. SPH mesh study models.
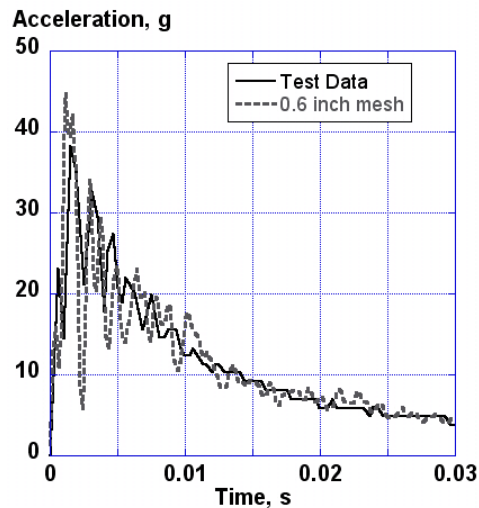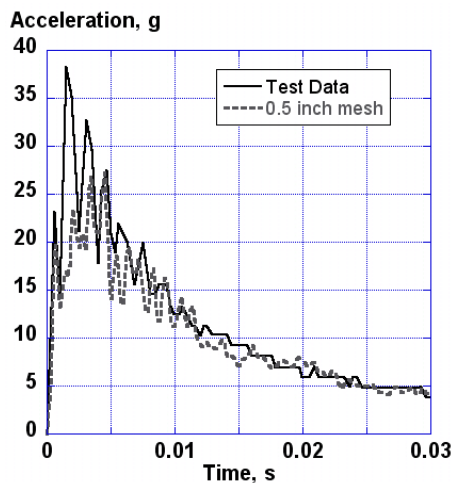
(a) 1.5- inch mesh.

(b) 1-inch mesh.

(c) 0.75-inch mesh.

(d) 0.6-inch mesh.

(e) 0.5-inch mesh.

Figure 22. SPH mesh study results.
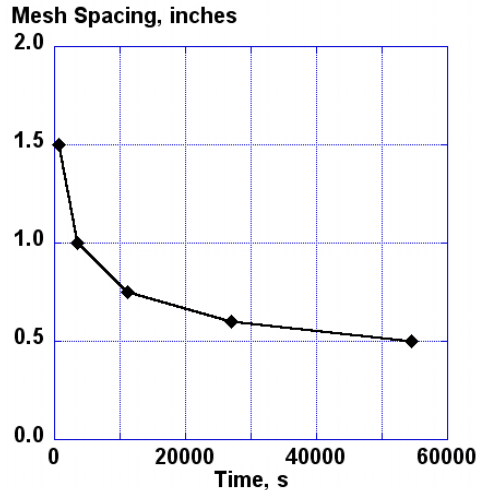
Mesh Spacing, inches

Figure 23. Mesh spacing versus solution time.

It should be noted that for most linear problems, mesh refinement should lead to a converged solution. However, for the impact contact problem, refining the mesh continuously may not provide a converged solution. Other factors such as contact algorithms, penalty stiffness, mesh ratios between the master part and the slave part may also affect the solutions. Also, experimental data may have inherent measurement errors and using these data to benchmark the finite element solutions may not be appropriate without fully characterizing and accounting for experimental uncertainties. In consideration of these factors, comparisons of the penetrometer test data with results from closed-form solutions were generated. Two closed-form solutions, one developed by von Karman [20] and the other developed by Wagner [21], of a rigid hemisphere impacting water were used to calculate peak accelerations based on the geometry and mass of the hemisphere and the density and depth of the water. These solutions are documented in Reference 22, in which the analytical approaches were used to evaluate water impacts of a space capsule into water. Based on the von Karman approach, a maximum acceleration of 26.5-g was calculated, and using the Wagner approach a peak acceleration of 40.5-g was determined. The actual experimental peak acceleration determined from the penetrometer drop test is 38-g, as shown in Figure 22. Thus, the results of the closed-form analyses bound the experimental response.

Concluding Remarks

An assessment of the ALE and SPH fluid-structure interaction methodologies available in LS-DYNA was conducted using test data from two vertical drop tests into water. The tests featured a 5-ft-diameter, 5-ft-long composite fuselage section, alone and with four blocks of a new composite honeycomb energy absorber, impacting a 15-ft-diameter, 42-in.-deep pool. The original objectives of the tests were to evaluate the energy absorption capabilities of the composite honeycomb concept for water impact and to generate test data for model validation, with the test of the stand-alone fuselage section acting as a baseline for comparison. Each test configuration was simulated using both ALE and SPH approaches in LS-DYNA. The composite honeycomb energy absorbers were represented using solid elements that were assigned a stress-strain response obtained from dynamic crush test data. For the ALE simulations, comparisons of pre-test predictions were correlated with test data, as well as post-test predictions that were generated from models incorporating a slight 1°-rolled attitude of the fuselage section at impact.

Initially, a cylindrical Eulerian mesh was used for the ALE simulations. Later, a refined 1-in. gradient mesh was used to study the influence of mesh density on the results. For the SPH simulations, comparisons were made for three different mesh densities having 3-, 2-, and 1.5-in. discretizations. The results of the SPH simulations prompted a separate study to investigate the influence of mesh density on the level of test-analysis correlation. For this study, the SPH method was used simulate a hemispherical penetrometer drop test into water. The major findings of this research were:

- The ALE method provided reasonable pre-test predictions of the floor level acceleration responses for both test configurations. For the test without energy absorbers, the predicted acceleration response, assuming a perfectly flat impact, was bounded by the test responses. Following the tests, the ALE model was updated by incorporating a 1°-roll attitude. The off-axis model gave accurate predictions of peak accelerations; however, the onset rate of acceleration did not match the test. For the test with energy absorbers, the pre-test predictions matched the acceleration onset rate; however, the peak value was over predicted by 3-g. The level of correlation improved when a 1°-roll attitude was incorporated into the model. These results demonstrate the importance of accounting for experimental eccentricities in the model to achieve optimal correlation.

- Initially, a cylindrical-shaped Euler model of air and water was used to simulate both test configurations. This mesh had a nominal element edge length of 2.7-in. in the region directly beneath the fuselage section. To study the influence of mesh discretization, a refined 1-in. gradient square-shaped mesh was used. The refined-mesh model did not show significant improvement in correlation.

- The SPH method was used to simulate both impact test configurations using three different (3-, 2-, and 1.5-in.) mesh densities. For the baseline test, the 3-in. SPH mesh provided the best correlation with experimental data. The results for the drop test of the fuselage section with DEA indicated that the 2-in. mesh spacing provided the best correlation with test data. Both findings were unexpected in that the finest SPH mesh did not yield the most accurate results.

- As a result of the SPH simulations, a separate study was conducted to further investigate the influence of mesh spacing. For this study, a hemispherical penetrometer drop test into water was simulated. Again, similar results were found in that the best correlation was obtained for an intermediate mesh spacing. This mesh density study clearly illustrates the importance of performing a mesh study using the SPH method and that it should not be assumed that by simply refining the mesh better results will be obtained.

- Even though peak accelerations were reduced by an order of magnitude when the deployable energy absorbers were used on the fuselage section, the primary mode of energy dissipation was through momentum transfer to the water. Very little crushing of the energy absorbers was observed. These results highlight the inherent difficulty in designing crashworthy structures for multi-terrain impact, and the need for robust simulation methods.

Acknowledgements

References

1. Jackson, K. E., Fuchs, Y. T., and Kellas, S., "Overview of the NASA Subsonic Rotary Wing Aeronautics Research Program in Rotorcraft Crashworthiness," Proceedings of the 11th ASCE Earth and Space Conference, March 3-5, 2008, Long Beach, CA.

2. Kellas S. and Jackson, K. E., "Deployable System for Crash-Load Attenuation," Proceedings of the 63rd AHS Forum, Virginia Beach, VA, May 1-3, 2007.

3. Kellas, S., and Jackson, K. E., "Multi-Terrain Vertical Drop Tests of a Composite Fuselage Section," Proceedings of the 64th AHS Forum, Montreal, Canada, April 29-May 1, 2008.

4. Hallquist, J. O., "LS-DYNA Keyword User's Manual, Version 971, Volumes 1 and 2," Livermore Software Technology Corporation, Livermore, CA, May 2007.

5. Noor, A. K., and Carden, H. C., editors, "Computational Methods for Crashworthiness," NASA Conference Publication 3223, October 1993.

6. Baldwin, M., "Final Report – Recommendations for Injury Prevention in Civilian Rotorcraft Accidents," TR-00016, Simula Technologies, Inc., February 29, 2000.

7. Sareen, A. K., Sparks, C., Mullins, B. R., Fasanella, E. L., and Jackson, K. E., "Comparison of Soft Soil and Hard Surface Impact Performance of a Crashworthy Composite Fuselage Concept," Proceedings of the AHS Forum 58, Montreal, Canada, June 11-13, 2002.

8. Fasanella, Edwin L., Jackson, Karen E., Sparks, Chad E., and Sareen, Ashish K., "Water Impact Test and Simulation of a Composite Energy Absorbing Fuselage Section," *Journal of the American Helicopter Society*, Vol. 50, No. 2, April 2005, pp. 150-164.

9. Witlin, G., Smith, M., and Richards, M., "Airframe Water Impact Analysis Using a Combined MSC/DYTRAN-DRI/KRASH Approach," Proceedings of the 53rd Annual Forum of the American Helicopter Society, Virginia Beach, VA, April 29 – May 1, 1997.

10. Tho, C. H., Sparks, C. E., and Sareen, A. K., "Hard Surface and Water Impact Simulations of Two Helicopter Sub-Floor Concepts," Proceedings of the 60th Annual Forum of the American Helicopter Society, Baltimore, MD, June 7-10, 2004.

11. Kohlgruber, D., Vigliotti, A., Weissberg, V., and Bartosch, H., "Numerical Simulation of a Composite Helicopter Sub-Floor Structure Subjected to Water Impact," Proceedings of the 60th Annual Forum of the American Helicopter Society, Baltimore, MD, June 7-10, 2004.

12. Pentecote, N. and Kindervater, C. M., "Airframe Water Impact Analysis Using a Local/Global Methodology," Proceedings of the AHS Forum 58, Montreal, Canada, June 11-13, 2002.

13. Fasanella, E. L., Jackson, K. E., and Kellas, S., "Soft Soil Impact Testing and Simulation of Aerospace Structures," Proceedings of the 10th LS-DYNA Users Conference, Dearborn, MI, June 8-10, 2008.

14.Hallquist, J. O., "LS-DYNA Theory Manual," Livermore Software Technology Corporation, Livermore, CA, March 2006.

15. Jackson, K. E., "Impact Testing and Simulation of a Crashworthy Composite Fuselage Concept," *International Journal of Crashworthiness,* 2001, Vol. 6, No 1, pp.107-121.

16. Fasanella, E. L., and Jackson, K. E., "Impact Testing and Simulation of a Crashworthy Composite Fuselage Section with Energy Absorbing Seats and Dummies," *Journal of the American Helicopter Society*, Vol. 49, No. 2, April 2004, pp. 140-148.

17. Lyle, K. H., Bark, L. W., and Jackson, K. E., "Evaluation of Test/Analysis Correlation Methods for Crash Applications," *Journal of the American Helicopter Society*, Vol. 47, No. 4, October 2002, pp. 219-232.

18. Fasanella, E. L., Jackson, K. E., Lyle, K. H., Sparks, C. E., and Sareen, A., "Multi-Terrain Impact Testing and Simulation of a Composite Energy Absorbing Fuselage Section," *Journal of the American Helicopter Society*, Vol. 52, No. 2, April 2007, pp 159-168.

19. Society of Automotive Engineers (SAE), Recommended Practice: Instrumentation for Impact Test – Part 1, Electronic Instrumentation, SAE J211/1, March 1995.

20. von Karman, T., "The Impact of Seaplane Floats during Landing," Technical Note 321, NACA, Washington D.C. 1929.

21. Wagner, H., "Über Stoss und Gleitvorgänge an der Oberfläche von Flüssigkeiten," *ZAMM* Vol. 12, 1932, pp. 193-215.

22. Wang, J. T. and Lyle, K. H., "Simulating Space Capsule Water Landing with Explicit Finite Element Method," AIAA-2007-1779, Proceedings of the 48th AIAA/ASME/ASCE/AHS/ASC Structures, Structural Dynamics, and Materials Conference, Honolulu, Hawaii, Apr. 23-26, 2007.